

# Untwisting the Boerdijk-Coxeter Helix

Robert L. Read [read.robert@gmail.com](mailto:read.robert@gmail.com)

**Abstract.** The Boerdijk-Coxeter helix (BC helix, or tetrahelix) is a face-to-face stack of regular tetrahedra forming a helical column. Considering the edges of these tetrahedra as structural members, the resulting structure is attractive and inherently rigid, and therefore interesting to architects, mechanical engineers, and roboticists. A formula is developed that matches the visually apparent helices forming the outer rails of the BC helix. This formula is generalized to a formula convenient to designers. Formulae for computing the parameters that give edge-length minimax-optimal tetrahelices are given, defining a continuum of tetrahelices of varying curvature. The endpoints of the optimality of this continuum are the BC helix and a structure of zero curvature, the *equitetrabeam*. Numerically finding the rail angle from the equation for pitch allows optimal tetrahelices of any pitch to be designed. An interactive tool for such design and experimentation is provided: <https://pubinv.github.io/tetrahelix/>. A formula for the inradius of optimal tetrahelices is given. Utility for static and variable geometry truss/space frame design and robotics is discussed.

**Key words.** Boerdijk-Coxeter helix, tetrahelix, robotics, tetrobot, unconventional robots, structural engineering, mechanical engineering, tensegrity, variable-geometry truss

18 AMS subject classifications. 51M15

**1. Introduction.** The Boerdijk-Coxeter helix[3] (BC helix), is a face-to-face stack of tetrahedra that winds about a straight axis. Because architects, structural engineers, and roboticians are inspired by and follow such regular mathematical models but can also build structures and machines of differing or even dynamically changing length, it is useful to develop the mathematics of structures formed from tetrahedra where we relax regularity.

The vertices of the tetrahedra lie upon three helices about the central axis. The Glussbot[11] (or Tetrobot)[8] uses the regularity of this geometry to make a tentacle-like robot that can crawl like a slug or mollusc. These modular robot systems uses mechanical actuators which can change their length, connected by special joints, such as the 3D printable Song-Kwon-Kim[15] joint in the case of the Glussbot, or the CMS joint[7], in the case of the Tetrobot, which allow many members to meet in a single point. Such machines can follow purely regular mathematical models such as the Boerdijk-Coxeter helix or the Octet Truss[4].

31       Buckminster Fuller called the BC helix a *tetrahelix*[5], a term now commonly used. In this  
 32 paper we reserve *BC helix* to mean the purely regular structure and use *tetrahelix* to refer to  
 33 any structure isomorphic to the BC helix.

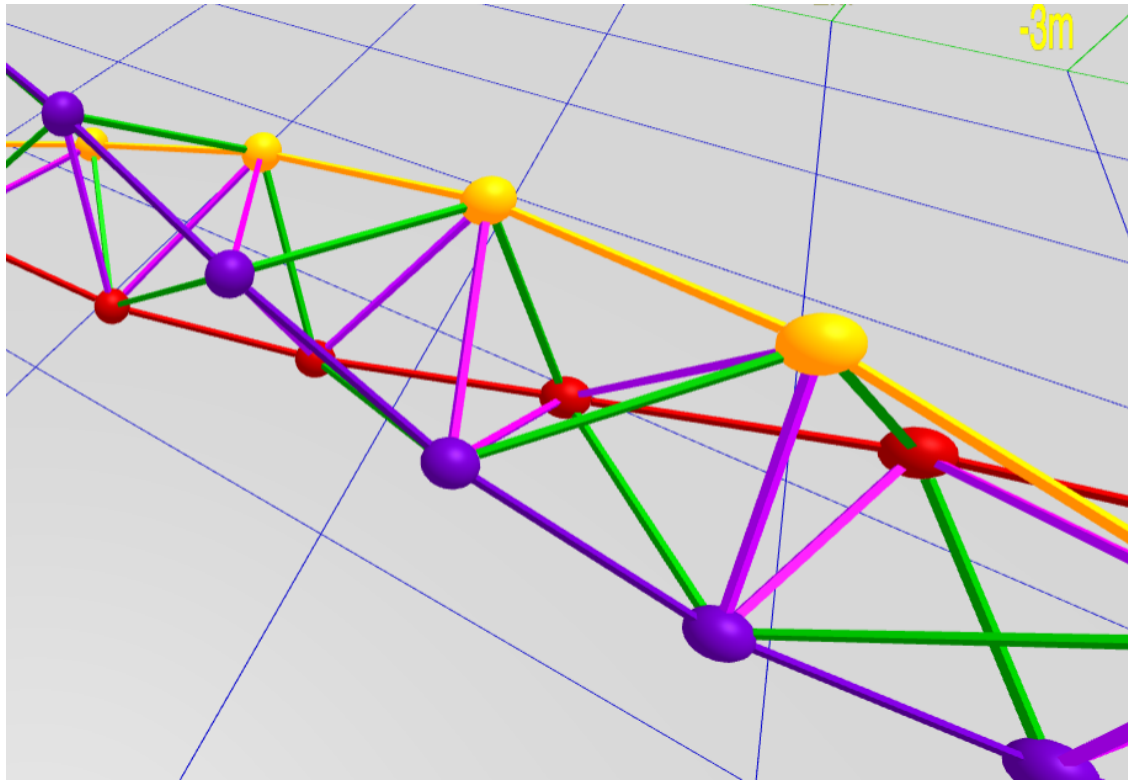


**Figure 1.** BC Helix Close-up (partly along axis)

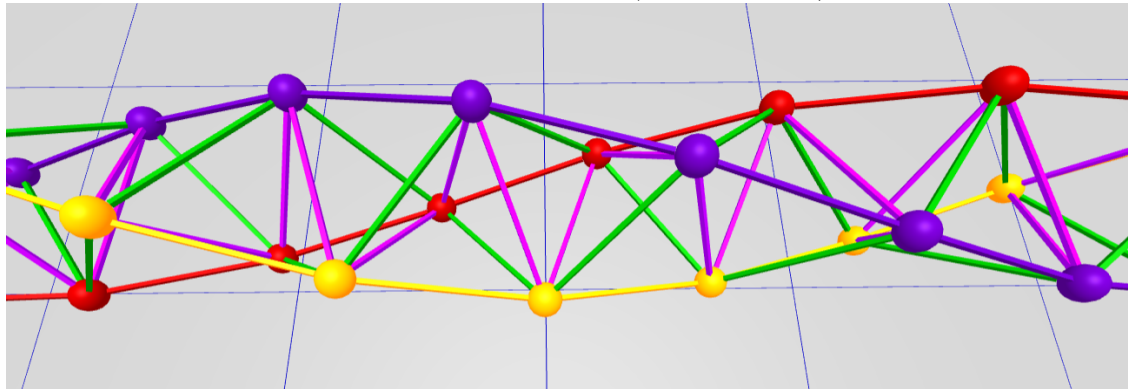


**Figure 2.** BC Helix Close-up (orthogonal)

34     Imagining Figure 2 as a static mechanical structure, we observe that it is useful to the  
 35 mechanical engineer or roboticist because the structure remains an inherently rigid, omni-  
 36 triangulated space frame, which is mechanically strong. Imagine further in Figure 2, that  
 37 each static edge was replaced with an actuator that could dynamically become shorter or  
 38 longer in response to electronic control, and the vertices were a joint that supported sufficient  
 39 angular displacement for this to be possible. An example of such a machine is a glussbot,  
 40 shown in Figure 12.

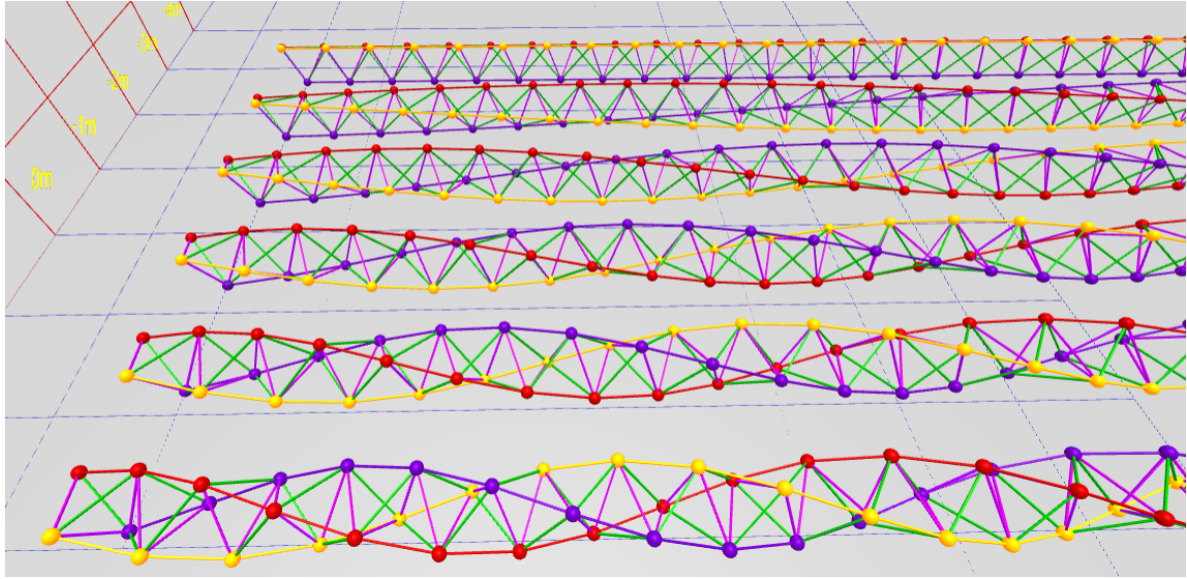


**Figure 3.** A Continuum of Tetrahelices

41     A BC helix does not rest stably on a plane. It is convenient to be able to “untwist” it and  
 42 to form a tetrahelix space frame that has a flat planar surface. By making length changes in a  
 43 certain way, we can untwist a tetrahelix to form a *tetrabeam* which has planar faces and has,  
 44 for example, an equilateral triangular profile. This paper develops the equations needed to  
 45 untwist the tetrahelix. All math developed here is available in JavaScript and demonstrated  
 46 by an interactive design website <https://pubinv.github.io/tetrahelix/>[12], from which Figure 2  
 47 and the figures below are taken.

48     Figure 3 displays a continuum of tetrahelices optimal in a certain sense, which is the result  
 49 of this paper. The closest helix is the BC helix, and the furthest is the equitetrabeam, defined  
 50 in section 6.

51     **2. A Designer’s Formulation of the BC Helix.** We would like to design nearly regular  
 52 tetrahelices with a formula that gives the vertices in space. Eventually we would like to design  
 53 nearly regular tetrahelices by choosing the lengths of a small set of members. In a space frame,  
 54 this is a static design choice; in a tetrobot, it is a dynamic choice that can be used to twist  
 55 the robot and/or exert linear or angular force on the environment.

56     Ideally we would have a simple formula for defining the nodes based on any curvature  
 57 or pitch we choose. It is a goal of this paper to relate these two approaches to generating a  
 58 tetrahelix continuum.

59     H.S.M Coxeter constructs the BC helix[3] as a repeated rotation and translation of the  
 60 tetrahedra, showing the rotation is:

$$61 \quad \theta_{bc} = \arccos(-2/3)$$

62 and the translation:

$$63 \quad h_{bc} = 1/\sqrt{10}$$

64  $\theta_{bc}$  is approximately  $0.37 \cdot 2\pi$  radians or 131.81 degrees. The angle  $\theta_{bc}$  is the rotation of  
 65 each tetrahedron, not the tetrahedra along a rail. In [Figure 2](#), each tetrahedron has either a  
 66 yellow, blue, or red outer edge or rail. That is, a blue-rail tetrahedron is rotated slightly more  
 67 than a 1/3 of a revolution to match the face of the yellow tetrahedra.

68 R.W. Gray's site[\[6\]](#), repeating a formula by Coxeter[\[3\]](#) in more accessible form, gives the

69 Cartesian coordinates  $\begin{bmatrix} x \\ y \\ z \end{bmatrix}$  for a counter-clockwise BC Helix in a right-handed coordinate  
 70 system:

$$71 \quad (1) \quad \mathbf{V}(n) = \begin{bmatrix} r_{bc} \cos n\theta_{bc} \\ r_{bc} \sin n\theta_{bc} \\ nh_{bc} \end{bmatrix}, \text{ where: } \begin{aligned} r_{bc} &= \frac{3\sqrt{3}}{10} \approx 0.5196 \\ h_{bc} &= 1/\sqrt{10} \approx 0.3162 \\ \theta_{bc} &= \arccos(-2/3) \end{aligned}$$

72 where  $n$  represents each integer numbered node in succession on every colored rail.

73 The apparent rotation of a vertex an outer-edge,  $\mathbf{V}(n)$  relative from  $\mathbf{V}(n+3)$  for any  
 74 integer  $n$  in [\(1\)](#), is  $3\theta_{bc} - 2\pi$ .

75 This formula defines a helix, but it is not any of the apparent helices, or *rail* helices, of the  
 76 BC helix, but rather one that winds three times as rapidly through all nodes. To a designer of  
 77 tetrahelices, it is more natural to think of the three helices which are visually apparent, that  
 78 is, those three which are closely approximated by the outer edges or rails of the BC helix. We  
 79 think of each of these three rails as being a different color: red, blue, or yellow. This situation  
 80 is illustrated in [Figure 4](#), wherein the black helix represents that generated by [\(1\)](#), and the  
 81 colored helices are generated by [\(2\)](#).

82 In order to develop the continuum of slightly irregular tetrahelices described in [section 7](#),  
 83 we need a formula that gives us the nodes of just one rail helix, denoted by color  $c$  and integer  
 84 node number  $n$ :

$$85 \quad (\forall n \in \mathbb{Z}, \forall c \in \{0, 1, 2\} : \mathbf{H}_{BCcolored}(n, c) = \mathbf{V}(3n + c))$$

86 Such a helix can be written:

$$87 \quad (2) \quad \mathbf{H}_{BCcolored}(n, c) = \begin{bmatrix} r_{bc} \cos ((3\theta_{bc} - 2\pi)n + c\theta_{bc}) \\ r_{bc} \sin ((3\theta_{bc} - 2\pi)n + c\theta_{bc}) \\ 3h_{bc}(n + c/3) \end{bmatrix}, \text{ where } \begin{aligned} r_{bc} &= \frac{3\sqrt{3}}{10} \\ h_{bc} &= 1/\sqrt{10} \\ \theta_{bc} &= \arccos(-2/3) \end{aligned}$$

88 In this formula, integral values of  $n$  may be taken as a node number for one rail and  
 89 used to compute its Cartesian coordinates. Allowing  $n$  to take non-integer values defines a  
 90 continuous helix in space which is close to the segmented polyline of the outer tetrahedra  
 91 edges, and equals them at integer values.

92 [Figure 4](#) illustrates this difference with a 7-tetrahedra BC helix, which is in fact the same  
 93 geometry as the robot illustrated in [Figure 12](#). Although the nodes coincide, [\(1\)](#) evaluated  
 94 at real values generates the black helix which runs through every node, and [\(2\)](#) defines the

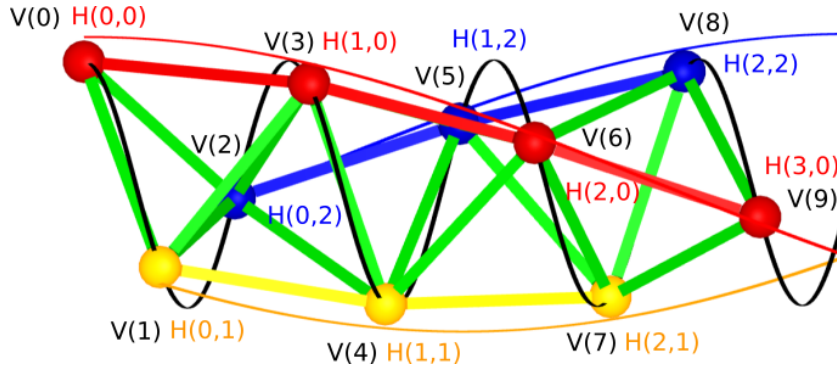


**Figure 4.** Rail helices ( $H$ ) vs. Coxeter/Gray helix ( $V$ )

95 red, yellow, and blue helices. (In this figure these rail helices have been rendered at a slightly  
96 higher radius than the nodes for clarity; in actuality the maximum distance between the  
97 continuous, curved helix and the straight edges between nodes is much smaller than can be  
98 clearly rendered.)

99 The quantity  $(3\theta_{bc} - 2\pi) \approx 35.43^\circ$  is the angular shift between  $\mathbf{V}(3n+c) = \mathbf{H}_{BCcolored}(n, c)$   
100 and  $\mathbf{V}(3(n+1)+c) = \mathbf{H}_{BCcolored}(n+1, c)$ . This quantity appears so often that we call it the  
101 “rail angle  $\rho$ ”. For the BC helix,  $\rho_{bc} = (3\theta_{bc} - 2\pi)$ .

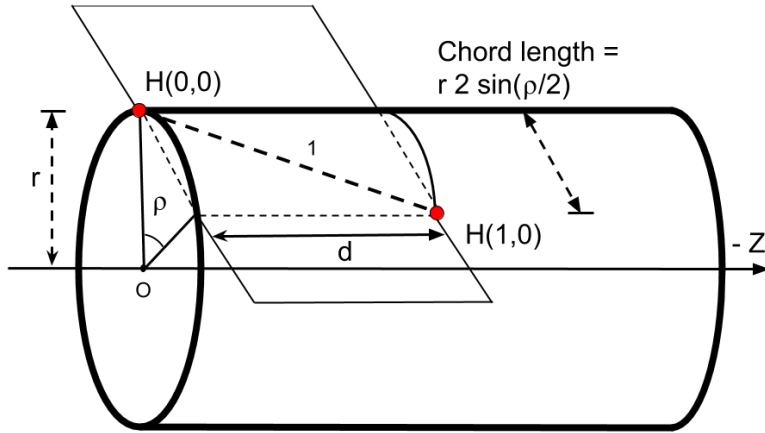


**Figure 5.** Rail Angle Geometry

102 Note in Figure 5 the  $z$ -axis travel for one rail edge is denoted by  $d$ . In (1) and (2),  
103 the variable  $h$  is used for one third of the distance we name  $d$ . We will later justify that  
104  $d = 3h$ . In this paper we assume the length of a rail is always 1 as a simplification, except in

105 proofs concerning rail length. (We make the rail length a parameter in our JavaScript code  
 106 in [https://github.com/PubInv/tetrahelix/blob/master/js/tetrahelix\\_math.js](https://github.com/PubInv/tetrahelix/blob/master/js/tetrahelix_math.js) [12].)

107 The  $\mathbf{H}_{BC\text{colored}}(n, c)$  formulation can be further clarified by rewriting directly in terms of  
 108 the rail angle  $\rho_{bc}$  rather than  $\theta_{bc}$ . Intuitively we seek an expression where  $c/3$  is multiplied by  
 109 a  $1/3$  rotation plus the rail angle  $\rho$ . We expand the expressions  $\theta_{bc}$  and  $\rho_{bc}$  in (2) and seek to  
 110 isolate the term  $c2\pi/3$ .

$$\begin{aligned} 111 \quad c\theta_{bc} &= \{\text{we aim for } 3 \text{ in denominator, so we split...}\} \\ 112 \quad (c/3)(3\theta_{bc}) &= \{\text{we want } 2\pi \text{ in numerator, so add canceling terms...}\} \\ 113 \quad (c/3)((3\theta_{bc} - 2\pi) + 2\pi) &= \{\text{definition of } \rho_{bc}\}... \\ 114 \quad (c/3)\rho_{bc} + c2\pi/3 &= \{\text{algebra...}\} \\ 115 \quad c(\rho_{bc} + 2\pi)/3 & \\ 116 \end{aligned}$$

118 This allows us to redefine:

$$119 \quad (3) \quad \mathbf{H}_{BC\text{colored}}(n, c) = \begin{bmatrix} r \cos \rho_{bc} n + c(\rho_{bc} + 2\pi)/3 \\ r \sin \rho_{bc} n + c(\rho_{bc} + 2\pi)/3 \\ (n + c/3)h_{bc} \end{bmatrix}, \text{ where } \begin{aligned} \rho_{bc} &= (3\theta_{bc} - 2\pi) \\ h_{bc} &= 1/\sqrt{10} \end{aligned}$$

120 Recall that  $c \in \{0, 1, 2\}$ , but  $n$  is continuous (rational or real-valued.) We can now assert  
 121 that in Figure 4 the black helix winds at  $\frac{3\theta_{bc}}{\rho_{bc}} \approx 11.16$  times the rate of a rail helix.

122 From this formulation it is easy to see that moving one vertex on a rail ( $\mathbf{H}_{BC\text{colored}}(n, c)$ )  
 123 to  $\mathbf{H}_{BC\text{colored}}(n + 1, c)$  for any  $n$  and  $c$ ) moves us  $\rho_{bc}$  radians around a circle. Since:

$$124 \quad \frac{2\pi}{\rho_{bc}} \approx 10.16$$

125 we can see that there are approximately 10.16 red, blue or yellow tetrahedra on one rail in a  
 126 single revolution.

127 The *pitch* of any tetrahelix, defined as the axial length of a complete revolution where  
 128  $\rho \neq 0$  is:

$$129 \quad (4) \quad p(\rho) = \frac{2\pi \cdot d}{\rho}$$

130 The pitch of the Boerdijk-Coxeter helix of edge length 1 is the length of three tetrahedra  
 131 times this number:

$$132 \quad \frac{3h_{bc} \cdot 2\pi}{\rho_{bc}} = \frac{6\pi}{\sqrt{10}\rho_{bc}} \approx 9.64$$

134 The pitch is less than the number of tetrahedra because the tetrahedra are not lined  
 135 up perfectly. It is a famous and interesting result that the pitch is irrational. A BC helix  
 136 never has two tetrahedra at precisely the same orientation around the  $z$ -axis. However, this

137 is inconvenient to designers, who might prefer a rational pitch. The idea of developing a  
138 rational period by arranging solid tetrahedra by relaxing the face-to-face matching has been  
139 explored[13]. We develop below slightly irregular edge lengths that support, for example, a  
140 pitch of precisely 12 tetrahedra in one revolution which would allow an architect to design a  
141 column having a basis and a capital in the same relation to the tetrahedra they touch at the  
142 bottom and top of the column.

143 **3. Optimal Tetrahelices are Triple Helices.** We use the term *tetrahelix* to mean any  
144 structure physically constructible of vertices and finite edges which is isomorphic to the BC  
145 helix and in which the vertices lie on three helices. By isomorphic we mean there is a one-  
146 to-one mapping between both vertices and edges in the two tetrahelices. One could consider  
147 various definitions of optimality for a tetrahelix, but the most useful to us as roboticists  
148 working with the Tetrobot concept is to minimize the maximum ratio between any two edge  
149 lengths, because the Tetrobot uses mechanical linear actuators with limited range of extension.

150 A *triple helix* is three congruent helices that share an axis. We show that optimal tetra-  
151 helices are in fact triple helices with the same radius, so that all vertices are on a cylinder.  
152 In, stages, we demonstrate that optimal tetrahelices:

- 153 1. have the same pitch,
- 154 2. have parallel axes,
- 155 3. share the same axis,
- 156 4. have the same radius,
- 157 5. have the same rail lengths,
- 158 6. have axially equidistant nodes, and therefore
- 159 7. are in fact triple helices.

160 Suppose that all three rails do not have the same pitch. Starting at any shortest edge  
161 between two rails, as we move from node to node away from our start edge the edge lengths  
162 between rails must always lengthen without bound, which cannot be optimal. So we are  
163 justified in talking about the *pitch* of the optimal tetrahelix as the pitch of its three rail  
164 helices, even though there are three such helices of equivalent pitch.

165 Similarly, if the axes are not parallel, there is an edge of unbounded length in the structure,  
166 so we do not consider such cases.

167 Define a *minimax edge-length optimal tetrahelix* or just an *optimal tetrahelix* to be a  
168 tetrahelix for which there exists no other tetrahelix with lower ratio of longest edge length to  
169 shortest edge length.

170 We wish to show that in an optimal tetrahelix, all vertices lie on the cylinder of radius  $r$ ,  
171 regardless of where they lie on the  $z$ -axis.

172 As a little lemma for the proof below, observe that a tetrahelix of zero radius, where all  
173 points lie on the same line, is not as optimal as a tetrahelix of a small radius. The edges  
174 between rails will be shorter than the rail edges, and moving them apart slightly lengthens  
175 the between-edge rails.

176 In the proof below we find useful to consider projection diagrams that are the axial pro-  
177 jection of a tetrahelix onto the  $XY$ -plane. ?? is an example of such a diagram.

178 **Lemma 1.** *If the rail angle  $0 < \rho < \pi$  is a rational multiple of  $\pi$ , then the projection of  
179 edges long a helix of that rail angle along the  $z$ -axis onto the  $XY$ -plane form a regular polygon*

180 of 3 or more sides, else they form a circle.

181 *Proof.* All points lying on a helix projected along the axis lie on a circle in the  $XY$ -plane.  
182 Helices are periodic in the  $z$  dimension modulo  $2\pi$ . If  $2\pi/\rho$  is irrational, the projection onto the  
183  $XY$ -plane will contain an unbounded number of points on a circle. Because  $\pi$  is transcendental  
184 and irrational,  $2\pi/\rho$  is rational if and only  $\rho = a\pi/b$ , where  $a$  and  $b$  are integers. Since  $\rho < \pi$ ,  
185  $a < b$ , and since  $\rho > 0$ ,  $a > 0$ . If and only if  $2\pi/\rho$  is rational, the projection onto the  $XY$ -plane  
186 will contain a finite number of points. The number of points in the projection is  $2b$  if  $a$  is  
187 odd, and  $b$  if  $a$  is even. This polygon has at least 3 sides, since either either  $\rho$  is irrational or  
188  $b > a$ , and therefore  $b \geq 2$ . If  $a/b = 1/2$ , the projection is a square, which has four sides. ■

189 **Theorem 2.** Any optimal tetrahelix with a rail angle of magnitude less than  $\pi$  has all three  
190 axes conincident.

191 *Proof.* Case 1: Suppose that  $\rho$  is zero. Each helix has zero curvature, that is, is a straight  
192 line. These lines are equivalent to some three helices, possibly with different radii, so long as  
193 there is a phase term in the defintion of the helix, as in (2). We later show the radii must be  
194 equivalent.

195 Case 2: Suppose that  $\rho$  is positive but less than  $\pi$ . In this case each rail helix has  
196 curvature. The projection of points in the  $XY$  plane creates a figure guaranteed to have  
197 point on either side of any line through the axis of such a helix, because the figure is either  
198 an  $n$ -gon or a circle. We show that the three helices share a common axis.

199 Without loss of generality define the Red helix to have its axis on the  $z$ -axis. Since either  
200 a Red-to-Yellow or a Red-to-Blue edge is either a minimum or a maximum, without loss of  
201 generatlity define the Blue helix to be a helix that has an edge connection to the Red helix  
202 that is either a maximum or a minimum. Let  $B'$  be a translation in the  $XY$ -plane of the  
203 blue helix  $B$  so that its axis is the  $z$ -axis and conincident with the red helix  $R$ . Let  $D$  be the  
204 distance between the axis of the Blue helix  $B$  and  $B'$ . We will show that if  $D > 0$  then  $B$   
205 “wobbles” in a way that cannot be optimal. Define a wobble vector by:

206 
$$\mathbf{W}(n) = \mathbf{B}(n) - \mathbf{B}'(n)$$

207 where  $\mathbf{B}(n)$  and  $\mathbf{B}'$  is the cartesian vector  $\begin{bmatrix} x \\ y \end{bmatrix}$  for the projection of the  $n$ th vertex of  $B$  and  
208  $B'$ . Note that  $\|\mathbf{R}(n) - \mathbf{B}'(n + k)\|$  (the Euclidean distance of the vertices) is a constant for  
209 any  $k$ , because  $R$  and  $B'$  have the same pitch and the same axis, even if they do not have the  
210 same radius.

211 **Figure 6** demonstrates illustrates this situation. Like most diagrams, it is over specific,  
212 in that the two circles are drawn of the same radius but we do not depend upon that in this  
213 proof. The diagram represents the projection along the  $z$  axis of points into the  $XY$ -plane.

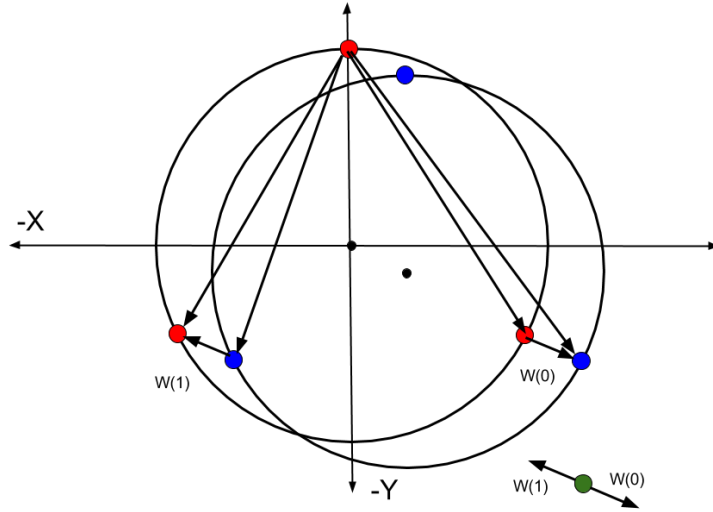


**Figure 6.** Wobble Vectors from Non-Coincident Axes

214 Since  $\rho < \pi$  by assumption, by [Lemma 1](#), the set of wobbles  $\{\mathbf{W}(n)\}$  for any  $n$  contains  
 215 at least three vectors, pointing in different directions. For any point not at the origin, at least  
 216 one of these vectors moves closer to the point and at least one moves further away.

217 The set of all lengths in the tetrahelix is a superset of:  $L = \{||\mathbf{R}(n) - \mathbf{B}(n)||\}$ , which  
 218 by our choice has at least one longest or shortest length. (Note this is just the Euclidean  
 219 distance formula written as a Euclidean norm.)  $L = \{||\mathbf{R}(n) - (\mathbf{B}'(n) + \mathbf{W}(n))||\}$  and so  
 220  $L = \{||(\mathbf{R}(n) - \mathbf{B}'(n)) - \mathbf{W}(n)||\}$ . But  $\mathbf{R}(n) - \mathbf{B}'(n)$  is a constant, so the minimax value of  
 221  $L$  is improved as  $||\mathbf{W}(n)||$  decreases. By our choice that there is a Blue-to-Red edge that is  
 222 either a maximum or a minimum, this improves the minimax value of the total tetrahelix.

223 This process can be carried out on both the Blue and Yellow helices (perhaps simulta-  
 224 neously) until  $\mathbf{W}(n)$  is zero for both, finding a tetrahelix of improved overall minimax value  
 225 at each step. So a tetrahelix is optimal only when  $\mathbf{W}(n) = 0$ , and therefore when  $D = 0$   
 226  $\mathbf{B}(n) = \mathbf{B}'(n)$ , and all three axes are coincident. ■

227 Now that we have show that axes are coincident and parallel and that the pitches are  
 228 the same for all helices, we can assert that any optimum tetrahelix can be generated with an  
 229 equation for helices:

230 (5) 
$$\mathbf{V}_{\text{triple}}(n, c) = \begin{bmatrix} r_c \cos(n\alpha + c2\pi/3 + \phi_c) \\ r_c \sin(n\alpha + c2\pi/3 + \phi_c) \\ \frac{d(n+c/3)}{3} \end{bmatrix}, \text{ where: } c \in \{0, 1, 2\}$$

231 which would not be much more complicated if the axes were not coincident. Note that we  
 232 have not yet show that the relationships of the radius  $r$  or the phase  $\phi$  for the three helies,  
 233 so we denoted them with a  $c$  subscript to show they are dependent on the color. We have

234 not yet investigated in the general case the relationships between  $\alpha$ ,  $r$ ,  $\phi$  and  $d$  in (5). In  
 235 section 4 we give a more specific version of this formula which generates optimal tetrahelices.  
 236 However, we observe that when  $\alpha = 0$ , the helices are degenerate, having curvature of 0, but  
 237 because of the  $\phi_c$  term, they are not collinear.

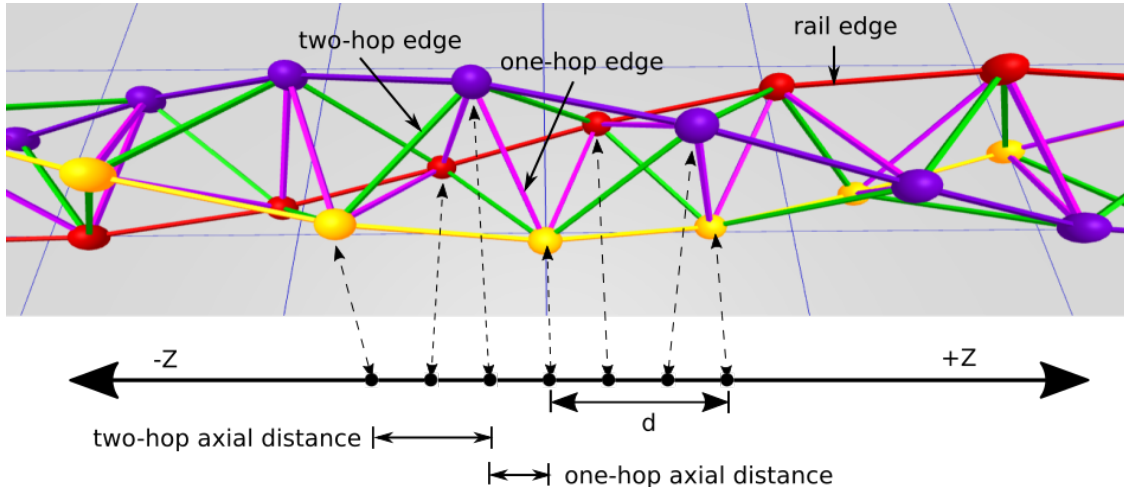


**Figure 7.** Edge Naming

238 In principle in any three helices generated with (5) has at most nine distinct edge length  
 239 classes. Each edge that connects two rails potentially has a longer length and shorter length  
 240 we denote with a + or -. So the classes are  $\{RR, BB, YY, RB_+, RB_-, BY_+, BY_-, RY_+, RY_-\}$ .  
 241 If when projecting all vertices onto the  $z$ -axis (dropping the  $x$  and  $y$  coordinates), the interval  
 242 defined by the  $z$  axis value of its endpoints contains no other vertices, we call it a *one-hop*  
 243 edge, and if it does contain another vertex we call it a *two-hop* edge, as illustrated in Figure 7.  
 244 Then there are 3 rail edges  $\{RR, BB, YY\}$ , 3 one-hop lengths  $\{RB_-, BY_-, RY_-\}$  between  
 245 each pair of 3 rails, and 3 two-hop lengths  $\{RB_+, BY_+, RY_+\}$  between each pair of 3 rails,  
 246 where the two-hop length is at least the one-hop length. However, if we generate the three  
 247 helices symmetrically with (5), many of these lengths will be the same. In fact, it is possible  
 248 that there will be only two distinct such classes.

249 **Theorem 3.** *Optimal tetrahelices have the same radii for all three helices.*

250 *Proof.* To prove this we exhibit a symmetric tetrahelix (not yet shown to be optimal)  
 251 which happens to be a triple helix, that has the property that all rail edges are equal to all  
 252 one-hop edges and all two-hop edges are equal. Observe that although we have not yet given  
 253 the formula for the radii of such a triple helix, we observe there are some values for  $r$  and  $\alpha$ ,  
 254 and  $\phi$  in (5) for which all the three helices are symmetrically and evenly spaced. Furthermore,  
 255 we can choose these values such that the three rail edges are of length unity and so that the  
 256 one-hop lengths are also all of length unity, and the two-hop lengths are slightly longer. We  
 257 call such a tetrahelix a two-class tetrahelix.

258 Now consider a tetrahelix in which the radius of one of the helices is different. By the

259 connections made in a tetrahelix, any increase to a radius increases both a one-hop and two-  
 260 hop distance, and any decrease likewise decreases two. Since there exists a tetrahelix which  
 261 has only two distinct classes of edge lengths, (the smaller being one-hop = rail, the larger  
 262 being the two-hop distance), the helix with a larger radius increases a longest edge without  
 263 increasing a shortest edges. Likewise, a helix with a smaller radius decreases a one-hop edge  
 264 without decreasing a two-hop edge. Therefore, a tetrahelix with different radii is not as good  
 265 as some two-class tetrahelix generated by (5), and so it not optimal. We have not yet proved  
 266 that a two-class tetrahelix is optimal, but it suffices to show that there exist such a better  
 267 tetrahelix to show that different radii imply a suboptimal tetrahelix. ■

268 Because an optimal tetrhelix has equivalent radii and equivalent pitch for all three helices,  
 269 it has equivalent rail edge lengths. Likewise, there is a single rail angle  $\rho$  that represents the  
 270 rotation of two nodes connected by a single rail edge, and it is the same for all three rails.

271 Now that we have shown that any optimal tetrahelix vertices are on helices of the same  
 272 axes and pitch, we see that the vertices of any optimal tetrahelix will lie on a cylinder, or a  
 273 circle when the axis dimension is projected out. Therefore it is reasonable to now speak of  
 274 the singular *radius r* of a tetrahelix as the radius of the cylinder. We can now go on to the  
 275 harder proof about where vertices occur along the  $z$ -axis.

276 We show that in fact the nodes must be distributed in even thirds along the  $z$ -axis, as in  
 277 fact they are in the regular BC helix.

278 However, we have already shown the rail lengths are equal in any optimal tetrahelix.

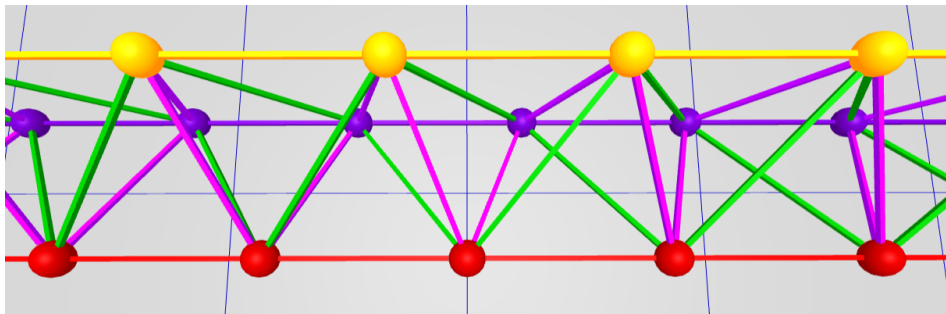


**Figure 8.** Equitetrabeam

279 **Figure 8** shows the equitetrabeam, which is defined in section 6, but also conveniently  
 280 illustrates the one-hop and two-hop edge definitions. The green edges are the two-hop edges  
 281 and the purple edges are the one-hop edges. Note that the green edges are slightly longer  
 282 than the purple edges. In 7, which depicts the BC helix, the two-hop and one-hop edges are  
 283 of equal length (but the projection onto the  $z$ -axis, the axial length, of the two-hop edge is  
 284 longer than the axial one-hop length.)

285 **Theorem 4.** *An optimal tetrahelix of any rail angle  $\rho < \pi$  is a triple helix with all vertices  
 286 evenly spaced at  $d/3$  intervals on the  $z$  axis. Any one tetrahedron in a tetrahelix has 1 rail  
 287 edge, 2 one-hop edges connected to the rail and 2 two-hop edges connected to the rail. The  
 288 edge opposite of the rail edge is a one-hop edge.*

289     *Proof.* Consider a tetrahelix in which the vertices are evenly spaced at  $d/3$  intervals on  
 290 the  $z$  axis. Every edge is either a rail edge, or it makes one hop, or it makes two hops. All of  
 291 the one-hop edges are equal length. All of the two-hop edges are equal length.

292     Every vertex is connected to 4 non-rail edges. There is a one-hop edge in both the positive  
 293 and negative  $z$  direction. Likewise there is a two-hop edge in both the positive and negative  
 294  $z$  direction. Let  $A$  be the set of edge lengths, which has only 3 members, represented by  
 295  $A = \{o, t, r\}$  for the one-hop, two-hop, and rail edge lengths.

296     Any attempt to perturb any rail in either  $z$  direction lengthens one two-hop edge to  $t'$ ,  
 297 where  $t' > t$  and shortens one one-hop edge  $o' < o$ . Let  $B = \{o', t'\} \cup A$  be the edge lengths  
 298 of such a perturbed tetrahelix. The minimax of  $B$  is greater than the minimax of  $A$  since  
 299 there is a single rail length which cannot be both greater than  $t'$  and  $o'$  and less than  $t'$  and  
 300  $o'$ . Therefore, any optimal tetrahelix has all one-hop edges between all rails equal to each  
 301 other, and all two-hop edges equal to each other, and the  $z$  distances between rails equal, and  
 302 therefore  $d/3$  from each other. ■

303     Note that based on [Theorem 4](#), there are only 3 possible lengths in an optimal tethrahelix,  
 304 and we are justified in classifying edge lengths as *rail*, *one-hop*, or *two-hop*. The one-hop edges  
 305 are the edges between rails that are closest on the  $z$ -axis, and the two-hop edges are those  
 306 that skip over a vertex.

307     Taking all of these results together, each helix in an optimal tetrahelix is congruent to the  
 308 others, shares an axis, is the same radius, and are evenly spaced axially. An optimal tetrahelix  
 309 is therefore a *triple helix*, (of a radius we have not yet demonstrated.)

310     **4. Parameterizing Tetrahelices via Rail Angle.** We seek a formula to generate optimal  
 311 tetrahelices that accepts a parameter that allows us to design the tetrahelix conveniently.  
 312 Please refer back to [Figure 5](#). The pitch of the helix is an obvious choice, but is not defined  
 313 when the curvature is 0, an important special case. The radius or the axial distance between  
 314 two nodes on the same rail are possible choices, but perhaps the clearest choice is to build  
 315 formulae that takes as their input the “rail angle”  $\rho$ . We define  $\rho$  to be the angle formed in  
 316 the X,Y plane  $\angle \mathbf{H}(0,0)O\mathbf{H}(0,1)$  projecting out the  $z$  axis and sighting along the positive  $z$   
 317 axis. In other words,  $\rho$  controls how far a rail edge of a tetrahelix deviates from being parallel  
 318 with the axis, or the “twistiness” of the tetrahelix. We use the parameter  $\chi = 1$  to indicate a  
 319 chirality of counter-clockwise, and  $\chi = -1$  for clockwise. We take our coordinate system to  
 320 be right-handed.

321     The quantities  $\rho, r, d$  are related by the expression:

$$322 \quad 1^2 = d^2 + (2r \sin \rho/2)^2 \\ 323 \quad (6) \quad d^2 = 1 - 4r^2(\sin \rho/2)^2$$

324

326     Checking the important special case of the BC helix, we find that this equation indeed  
 327 holds true (treating  $d$  in this equation as  $3h_{bc}$  as defined by Gray and Coxeter, that is,  
 328  $d_{bc} = 3h_{bc}$ , where they are using  $h$  for the axial height from one node to the next of a different  
 329 color, but we use  $d$  to mean distance between nodes of the same color.)

330 The rail angle  $\rho$  also has the meaning that  $2\pi/\rho$  is the number of tetrahedra in a full  
 331 revolution of the helix.

332 In choosing  $\rho$ , one greatly constrains  $r$  and  $d$ , but does not completely determine both of  
 333 them together, so we treat both as parameters.

334 Rewriting our formulation in terms of  $\rho$ :

$$335 \quad (7) \quad \mathbf{H}_{general}(\chi, n, c, \rho, d_\rho, r_\rho) = \begin{bmatrix} r_\rho \cos(\chi \cdot (n\rho + c(\rho + 2\pi)/3)) \\ r_\rho \sin(\chi \cdot (n\rho + c(\rho + 2\pi)/3)) \\ d_\rho(n + c/3) \end{bmatrix}$$

336 where:  $1 = d_\rho^2 + 4r_\rho^2(\sin \rho/2)^2$   
 337  $\chi \in \{-1, 1\}$

338  $\mathbf{H}_{general}$  forces the user to select three values:  $\rho$ ,  $r_\rho$ , and  $d_\rho$  satisfying (6).  
 339 Note that when  $\rho = 0$  then  $d_\rho = 1$ , but  $r_\rho$  is not determined by (6).

340 **Theorem 5.** For rail angles of magnitude at most  $\rho_{bc}$ , tetrahelices generated by  $\mathbf{H}_{general}$   
 341 are optimal in terms of minimum maximum ratio of member length when radius is chosen so  
 342 that the length of the one-hop edge is equal to the rail length.

343 **Proof.** By Theorem 4, we can compute the (at most) three edge-lengths of an optimal  
 344 tetrahelix by formula universally quantified by  $n$  and  $c$ :

$$345 \quad \text{rail} = \|\mathbf{H}_{general}(n, c, \rho, d_\rho, r) - \mathbf{H}_{general}(n+1, c, \rho, d_\rho, r)\| = 1$$

$$346 \quad \text{one-hop} = \|\mathbf{H}_{general}(n, c, \rho, d_\rho, r) - \mathbf{H}_{general}(n, c+1, \rho, d_\rho, r)\|$$

$$347 \quad \text{two-hop} = \|\mathbf{H}_{general}(n, c, \rho, d_\rho, r) - \mathbf{H}_{general}(n, c+2, \rho, d_\rho, r)\|$$

348

350 This syntax just represents the Euclidean distance formula.

$$351 \quad \text{one-hop} = \|\mathbf{H}_{general}(n, c, \rho, d_\rho) - \mathbf{H}_{general}(n, c+1, \rho, d_\rho), r\|$$

$$352 \quad \text{one-hop} = \sqrt{\frac{d_\rho^2}{9} + r^2(\sin^2(\rho/3 + \frac{2\pi}{3}) + (1 - \cos(\rho/3 + \frac{2\pi}{3}))^2)}$$

353 but:  $d_\rho^2 = 1 - 4r^2(\sin(\rho/2)^2)$  ...so we substitute:

$$354 \quad \text{one-hop} = \sqrt{\frac{1}{9} + r^2(-\frac{4(\sin^2(\rho/2))}{9} + \sin^2(\rho/3 + \frac{2\pi}{3}) + (1 - \cos(\rho/3 + \frac{2\pi}{3}))^2)}$$

355

357 By similar algebra and trigonometry:

$$358 \quad \text{two-hop} = \sqrt{\frac{4}{9} + r^2(-\frac{16(\sin^2(\rho/2))}{9} + \sin^2(2\rho/3 + \frac{4\pi}{3}) + (1 - \cos(2\rho/3 + \frac{4\pi}{3}))^2)}$$

359

361 By definition of minimax edge length optimality, we are trying to minimize:

362

$$\frac{\max\{1, \text{one-hop}(r), \text{two-hop}(r)\}}{\min\{1, \text{one-hop}(r), \text{two-hop}(r)\}}$$

363 But since  $\text{two-hop}(r) \geq \text{one-hop}(r)$ , this is equivalent to:

364

$$\frac{\max\{1, \text{two-hop}(r)\}}{\min\{1, \text{one-hop}(r)\}}$$

365 This quantity will be equal to one of:

366 (8) 
$$\frac{\text{two-hop}(r)}{1}, \frac{1}{\text{one-hop}(r)}, \frac{\text{two-hop}(r)}{\text{one-hop}(r)}$$

367 We know that both  $\text{one-hop}(r)$  and  $\text{two-hop}(r)$  increase monotonically and continuously  
368 with increasing  $r$ . By inspection it seems likely that we will minimize this set by equating  
369  $\text{one-hop}(r)$  or  $\text{two-hop}(r)$  to 1, but to be absolutely sure and to decide which one, we must  
370 examine the partial derivative of the ratio  $\frac{\text{two-hop}(r)}{\text{one-hop}(r)}$  in this range.

371 Although complicated, we can use Mathematica to investigate the partial derivative of  
372 the  $\frac{\text{two-hop}(r)}{\text{one-hop}(r)}$  with respect to the radius to be able to understand how to choose the radius to  
373 form the minimax optimum.

374 Let:

375

$$f_\rho = -\frac{4(\sin^2(\rho/2))}{9}$$

376

$$g_\rho = -\frac{16(\sin^2(\rho/2))}{9}$$

378

$$j_\rho = \sin^2(\rho/3 + \frac{2\pi}{3}) + (1 - \cos(\rho/3 + \frac{2\pi}{3}))^2$$

379

$$k_\rho = (\sin^2(2\rho/3 + \frac{4\pi}{3}) + (1 - \cos(2\rho/3 + \frac{4\pi}{3}))^2)$$

381 Then:

382

$$\frac{\text{two-hop}(r)}{\text{one-hop}(r)} = \frac{\sqrt{\frac{4}{9} + r^2(g_\rho + j_\rho)}}{\sqrt{\frac{1}{9} + r^2(f_\rho + k_\rho)}}$$

384 By graph inspection using Mathematica (<https://github.com/PubInv/tetrahelix/blob/master/tetrahelix.nb>), we see the partial derivative of this with respect to radius  $r$  is always  
385 negative, for any  $\rho \leq \rho_{bc}$ . (When the rail angle approaches  $\pi$ , corresponding to going almost to  
386 the other side of the tetrahelix, this is not necessarily true, hence the limitation in our state-  
387 ment of the theorem is meaningful.) Since the partial derivative of  $\text{two-hop}(r)/\text{one-hop}(r)$

389 with respect to the radius  $r$  is negative for all  $\rho$  up until  $\rho_{bc}$ , this ratio goes down as the radius  
 390 goes up, and we minimize the maximum edge-length ratio by choosing the largest radius up  
 391 until one-hop = 1, the rail-edge length. If we attempted to increase the radius further we  
 392 would not be optimal, because the ratio  $\frac{\text{two-hop}(r)}{1}$  would because the largest ratio in our set  
 393 of ratios (8).

394 Therefore we decrease the minimax length of the whole system as we increase the radius  
 395 up to the point that the shorter, one-hop distance is equal to the rail-length, 1. Therefore, to  
 396 optimize the whole system so long as  $\rho \leq \rho_{bc}$ , we equate one-hop to 1 to find the optimum  
 397 radius:

$$398 \quad 1 = \sqrt{\frac{1}{9} + r_{opt}^2 \left( -\frac{4(\sin^2(\rho/2))}{9} + \sin^2(\rho/3 + \frac{2\pi}{3}) + (1 - \cos(\rho/3 + \frac{2\pi}{3}))^2 \right)}$$

$$399 \quad (9) \quad r_{opt} = \frac{2}{\sqrt{\frac{9}{2} \cdot (\sqrt{3}\sin(\rho/3) + \cos(\rho/3)) + \cos(\rho) + 8}}$$

400

402 We can now give a formula for  $d_{opt}$  computed from  $\rho, r_{opt}$  via the rail angle equation (6):

$$403 \quad d_{opt}^2 = 1 - 4 \left( \frac{2}{\sqrt{\frac{9}{2} \cdot (\sqrt{3}\sin(\rho/3) + \cos(\rho/3)) + \cos(\rho) + 8}} \right)^2 (\sin \rho/2)^2$$

$$404 \quad d_{opt}^2 = 1 - \frac{16(\sin \rho/2)^2}{9(\sqrt{3}\sin(\rho/3) + \cos(\rho/3)) + \cos(\rho) + 8}$$

$$405 \quad (10) \quad d_{opt} = \sqrt{1 - \frac{16 \sin^2(\rho/2)}{\cos(\rho) + 9(\sqrt{3}\sin(\rho/3) + \cos(\rho/3)) + 8}}$$

406

408 Thus, by computing  $r_{opt}$  and  $d_{opt}$  as a function of  $\rho$  from this equation, we can construct  
 409 minimax optimal tetrahelix for an  $0 \leq \rho \leq \rho_{bc}$ . ■

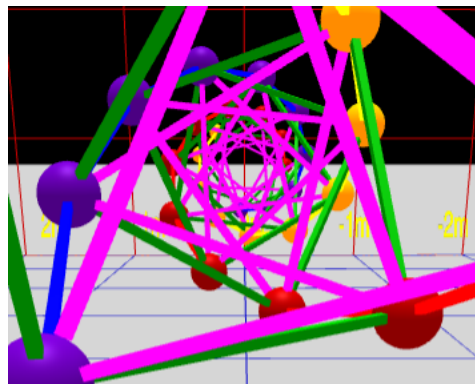


**Figure 9.** Axial view of a BC-Helix

**5. The Inradius.** Since the axes are parallel, we may define the *inradius*, represented by the letter  $i$ , of a tetrahelix to be the radius of the largest cylinder parallel to this axis that is surrounded by each tetrahelix and pentrated by no edge.

If we look down the axis of an optimal tetrahelix as shown in Figure 9, it happens that only the one-hop edges (rendered in purple in our software) comes closest to the axis. In other words, they define the radius of the incircle of the projection, or the radius of a cylinder that would just fit inside the tetrahelix. A formula for the inradius of the tetrahelix is useful if you are designing it as a structure that bears something internally, such as a firehose, a pipe, or a ladder for a human. The inradius  $r_{in}(\rho)$  of an optimal tetrahelix is a remarkably simple function of the radius  $r$  and the rail angle  $\rho$ :

$$420 \quad (11) \qquad r_{in}(\rho) = r \sin \frac{\pi - \rho}{6}$$

421 Which can be seen from the trigonometry of a diagram of the projected one-hop edges con-  
422 necting four sequentially numbered vertices:

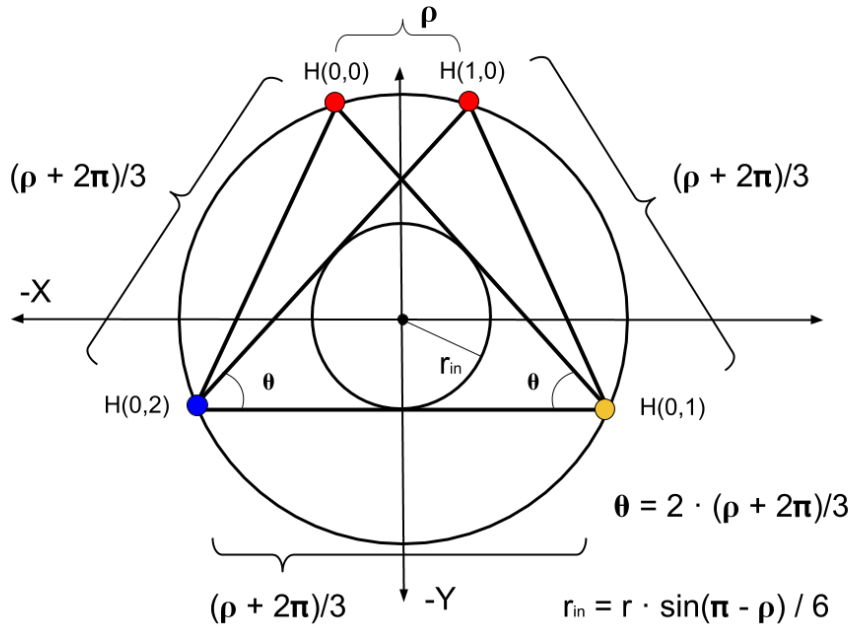


**Figure 10.** General One-hop Projection Diagram

From this equation with the help of symbolic computation we observe that inradius of the BC helix of unit rail length is  $r_{in}(\rho_{bc}) = \frac{3}{10\sqrt{2}} \approx 0.21$ .

**6. The Equitetrabeam.** Just as  $\mathbf{H}_{\text{general}}$  constructs the BC helix (with careful and non-obvious choices of parameters) which is an important special case due to its regularity, it constructs an additional special (degenerate) case when the rail angle  $\rho = 0$  and  $d = 1$  (the

428 edgelength), where the cross sectional area is an equilateral triangle of unchanging orientation,  
 429 as shown in [Figure 8](#) and at the rear of [Figure 3](#). We call this the *equitetrabeam*. It is not  
 430 possible to generate an equitetrabeam from [\(1\)](#) without the split into three rails introduced  
 431 by [\(2\)](#) and completed in [\(7\)](#).

432     **Corollary 6.** *The equitetrabeam with minimal maximal edge ratio is produced*  
 433 *by  $\mathbf{H}_{\text{general}}$  when  $r = \sqrt{\frac{8}{27}}$ .*

434     *Proof.* Choosing  $d = 1$  and  $\rho = 0$  we use Equation [\(9\)](#) to find the radius of optimal  
 435 minimax difference.

436     Substituting into [\(7\)](#):

$$437 \quad \text{one-hop} = \sqrt{\frac{1}{9} + 3r^2}$$

438

440     Then:

$$441 \quad 1 = \sqrt{\frac{1}{9} + 3r^2} \quad \text{solved by...}$$

$$442 \quad r = \sqrt{\frac{8}{27}} \quad \approx 0.54$$

443

445     This radius<sup>1</sup> produces a two-hop rail length of  $\frac{2}{\sqrt{3}}$ . The difference between this and 1 is  
 446  $\approx 15.47\%$ . The inradius of the equitetrabeam of unit rail length from both Equation [\(11\)](#) and  
 447 the fact that the inradius of an equilateral triangle is half the circumradius is  $\sqrt{\frac{8}{27}}/2$ , or  $\frac{\sqrt{6}}{9}$ .

448     In [Figure 3](#), the furthest tetrahelix is the optimal equitetrabeam. [Figure 8](#) is a closeup of  
 449 an equitetrabeam.

450     To the extent that we value tetrabeams (that is, tetrahelices with a rail angle of 0, and  
 451 therefore zero curvature and curvature) as mathematical or engineering objects, we have  
 452 motivated the development of  $\mathbf{H}_{\text{general}}$  as a transformation of  $\mathbf{V}(n)$  defined by Equation [\(1\)](#)  
 453 from Gray and Coxeter. It is difficult to see how the  $\mathbf{V}(n)$  formulation could ever give rise  
 454 to a continuum producing the tetrabeam, since setting the angle in that equation to zero can  
 455 produce only collinear points.

456     The equitetrabeam may possibly be a novel construction. The fact that 6 members meet  
 457 in a single point would have been a manufacturing disadvantage that may have dissuaded  
 458 structural engineers from using this geometry. However, the advent of additive manufacturing,  
 459 such a 3D printing, and the invention of two distinct concentric multimember joints[\[15, 7\]](#) has  
 460 improved that situation.

461     Note that the equitetrabeam has chirality, which becomes important in our attempt to  
 462 build a continuum of tetrahelices.

---

<sup>1</sup>Another interesting but non-optimal solution is derived by setting  $(\text{one-hop} + \text{two-hop})/2 = 1$ , occurs at  $r = \sqrt{35}/4$  which produces three length classes of  $11/12, 12/12, 13/12$ .

463     **7. An Untwisted Continuum.** We observe that Equations (9) and (10) compute  $r_{opt}$   
 464 and  $d_{opt}$  which create an optimal tetrahelix for any rail angle  $\rho$  between 0, which gives the  
 465 equitetrabeam and  $\rho_{bc} \approx 35.43^\circ$ , which gives the BC helix.

466     Because the equitetrabeam which has a rail angle of 0 still has chirality, that is, one still  
 467 must decide to connect the one-hop edge to the clockwise or the counter-clockwise node, it is  
 468 not possible to build a smooth continuum where  $\rho$  transitions from positive to negative which  
 469 remains optimal. One can use a negative  $\rho$  in  $\mathbf{H}_{general}$  but it does not produce minimax  
 470 optimal tetrahelices. In other words, untwisting a counter-clockwise tetrahelix to rail angle 0  
 471 and then going even further does produce a clockwise tetrahelix, but one in which the one-hop  
 472 and two-hop lengths in the wrong places (that is, two-hop becomes shorter than one-hop.)  
 473 Likewise,  $\rho > \rho_{bc}$  generates a tetrahelix, but minimax optimality is not guaranteed by  $\mathbf{H}_{general}$ .

474     The pitch of a helix (see (4), for a fixed  $z$ -axis travel  $d$ , is trivial. However, if one is  
 475 computing  $z$ -axis travel from (10) the pitch is not simple. It increases monotonically and  
 476 smoothly with decreasing  $\rho$ , so Equation (4) can be easily solved numerically with a Newton-  
 477 Raphson solver, as we do on our website. For a pitch at least  $p \geq \frac{3\sqrt{2}\pi}{\sqrt{5}\rho_{bc}} \approx 9.64$ , using (10)  
 478 produces minimax optimal tetrahelices.

479     In this way a rail angle can be chosen for any desired (sufficiently large) pitch, yield the  
 480 optimum radius, one-hop, and two-hop lengths an engineer needs to construct a physical  
 481 structure.

482     The curvature of a rail helix is formally given by:

483 (12) 
$$\frac{|r_\rho|}{r_\rho^2 + (d_\rho/\rho)^2}$$

484 which goes to 0 as  $\rho$  approaches 0 (the equitetrabeam.) As  $\rho$  increase up to  $\rho_{bc}$  the curvature  
 485 increases smoothly until the BC Helix is reached.

486     Perhaps surprisingly, the optimal untwisting is accomplished only by changing the length  
 487 of the two-hop member, leaving the one-hop member and rail length equivalent within this  
 488 continuum.<sup>2</sup> However, it should be noted that an engineer or architect may also use  $\mathbf{H}_{general}$   
 489 directly and interactively, and that minimax length optimality is a mathematical starting point  
 490 rather than the final word on the beauty and utility of physical structures. For example, a  
 491 structural engineer might increase radius past optimality in order to resist buckling.

492     If an equitetrabeam were actually used as a beam, an engineer might start with the  
 493 optimal tetrabeam and dilate it in one dimension to “deepen” the beam. Similarly, simple  
 494 length changes curve the equitetrabeam into an “arch”. The “colored” approach of (7) exposes  
 495 these possibilities more than the approach of (1).

496     Trusses and space frames remain an important design field in mechanical and structural  
 497 engineering[10], including deployable and moving trusses[2].

---

<sup>2</sup>Before deriving Equation (9), we created a continuum by using a linear interpolation between the optimal radius for the Equitetrabeam and the BC Helix. This minimax optimum of this simpler approach was at most 1% worse than the optimum computed by (9).

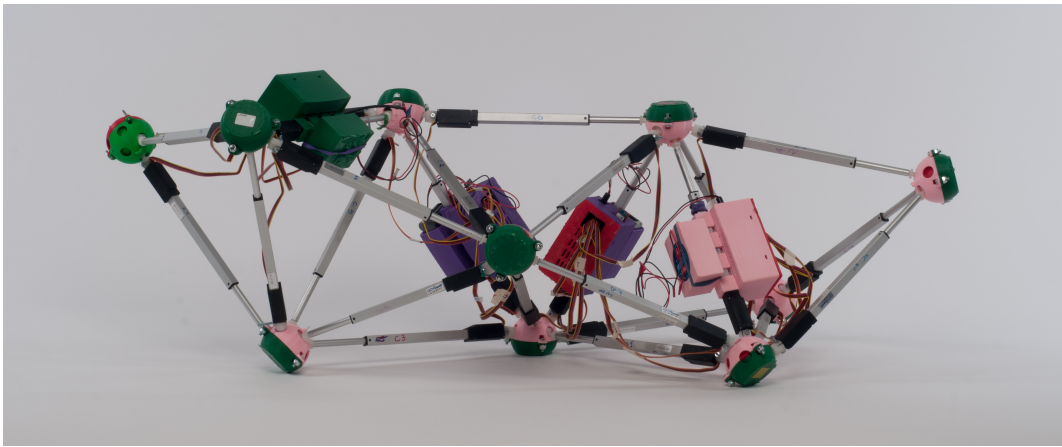


**Figure 11.** *Glussbot in relaxed, or BC helix configuration*

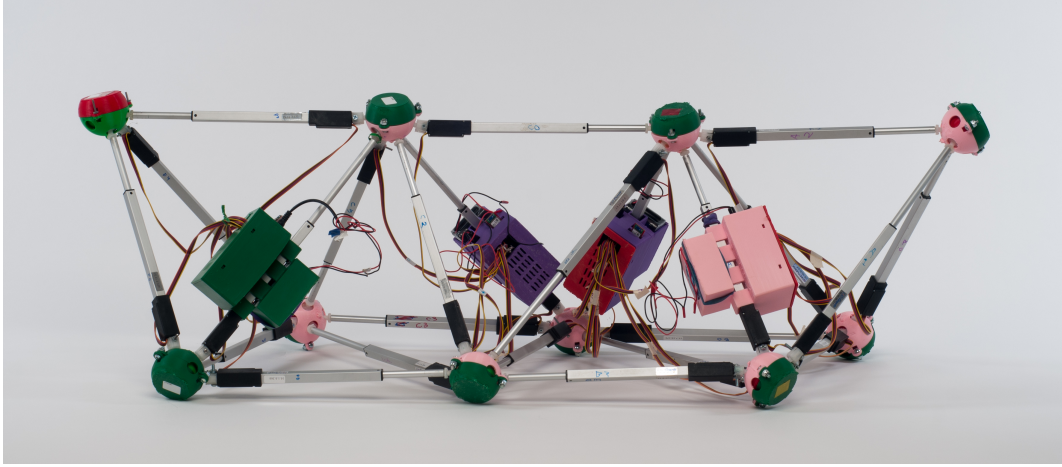


**Figure 12.** *The Equitetrabeam: Fully Untwisted Glussbot in Hexapod Configuration*

498     **8. Utility for Robotics.** Starting twenty years ago, Sanderson[14], Hamlin,[8], Lee[9], and  
 499 others created a style of robotics based on changing the lengths of members joined at the  
 500 center of a joint, thereby creating a connection to pure geometry. More recently NASA has  
 501 experimented with tensegrities[1], a different point in the same design spectrum. These fields  
 502 create a need to explore the notion of geometries changing over time, not generally considered  
 503 directly by pure geometry.

504     As suggested by Buckminster Fuller, the most convenient geometries to consider are those  
 505 that have regular member lengths, in order to facilitate the inexpensive manufacture and  
 506 construction of the robot. In a plane, the octet truss[4] is such a geometry, but in a line, the  
 507 Boerdijk-Coxeter helix is a regular structure.

508     However, a robot must move, and so it is interesting to consider the transmutations of  
 509 these geometries, which was in fact the motivation for creating the equitetrabeam.

510     **Theorem 7.** *By changing only the length of the longer members that connect two distinct  
 511 rails (the two-hop members), we can dynamically untwist a tetrobot forming the Boerdijk-*

512 Coxeter configuration into the equitetrabeam which rests flat on the plane.

513 *Proof.* Proof by our computer program that does this using Equation (7) applied to the  
514 7-tet Tetrobot/Glussbot.

515 By untwisting the tetrahelix so that it has a planar surface resting on the ground, we may  
516 consider each vertex touching the ground a foot or pseudopod. A robot can thus become a  
517 hexapod or  $n$ -pod robot, and the already well-developed approaches to hexapod gaits may be  
518 applied to make the robot walk or crawl.

519 **9. Conclusion.** The BC Helix is the end point of a continuum of tetrahelices, the other end  
520 point being an untwisted tetrahelix with equilateral cross section, constructed by changing the  
521 length of only those members crossing the outside rails after hopping over the nearest vertex.  
522 Under the condition of minimum maximum length ratios of all members in the system, all  
523 such tetrahelices have vertices evenly spaced along the axis generated by a simple equation  
524 and are in fact triple helices. A machine, such as a robot or a variable-geometry truss, that  
525 can change the length of its members can thus twist and untwist itself by changing the length  
526 of the appropriate members to achieve any point in the continuum. With a numeric solution,  
527 a designer may choose a rotation angle and member lengths to obtain a desired pitch.

528 **10. Contact and Getting Involved.** The Gluss Project <http://pubinv.github.io/gluss/> is  
529 part of Public Invention <https://pubinv.github.io/PubInv/>, a free-libre, open-source research,  
530 hardware, and software project that welcomes volunteers. It is our goal to organize projects for  
531 the benefit of all humanity without seeking profit or intellectual property. To assist, contact  
532 [read.robert@gmail.com](mailto:read.robert@gmail.com).

533

## REFERENCES

- 534 [1] *NTRT - NASA Tensegrity Robotics Toolkit.* <https://ti.arc.nasa.gov/tech/asr/intelligent-robotics/tensegrity/ntrt/>. Accessed: 2016-09-13.
- 535 [2] J. CLAYPOOL, *Readily configured and reconfigured structural trusses based on tetrahedrons as modules*,  
536 Sept. 18 2012, <https://www.google.com/patents/US8266864>. US Patent 8,266,864.
- 537 [3] H. COXETER ET AL., *The simplicial helix and the equation  $\tan(n \theta) = n \tan(\theta)$* , Canad. Math. Bull, 28  
538 (1985), pp. 385–393.
- 539 [4] R. FULLER, *Synergetic building construction*, May 30 1961, <https://www.google.com/patents/US2986241>.  
540 US Patent 2,986,241.
- 541 [5] R. FULLER AND E. APPLEWHITE, *Synergetics: explorations in the geometry of thinking*, Macmillan, 1982,  
542 <https://books.google.com/books?id=G8baAAAAMAAJ>.
- 543 [6] R. W. GRAY, *Tetrahelix data*. <http://www.rwgrayprojects.com/rbfnotes/helix/helix01.html>, <http://www.rwgrayprojects.com/rbfnotes/helix/helix01.html> (accessed Accessed: 2017-04-08).
- 544 [7] G. J. HAMLIN AND A. C. SANDERSON, *A novel concentric multilink spherical joint with parallel robotics*  
545 *applications*, in Proceedings of the 1994 IEEE International Conference on Robotics and Automation,  
546 May 1994, pp. 1267–1272 vol.2, <https://doi.org/10.1109/ROBOT.1994.351313>.
- 547 [8] G. J. HAMLIN AND A. C. SANDERSON, *Tetrobot: A Modular Approach to Reconfigurable Parallel*  
548 *Robotics*, Springer Science & Business Media, 2013, <https://play.google.com/store/books/details?id=izrSBwAAQBAJ> (accessed 2017-04-08).
- 549 [9] W. H. LEE AND A. C. SANDERSON, *Dynamic rolling locomotion and control of modular robots*, IEEE  
550 Transactions on robotics and automation, 18 (2002), pp. 32–41.
- 551 [10] M. MIKULAS AND R. CRAWFORD, *Sequentially deployable maneuverable tetrahedral beam*, Dec. 10 1985,  
552 <https://www.google.com/patents/US4557097>. US Patent 4,557,097.

- 556 [11] R. L. READ, *Gluss = Slug + Truss*. Unpublished preprint, <https://github.com/PubInv/gluss/blob/gh-pages/doc/Gluss.pdf> (accessed 2016-10-27).
- 557 [12] R. L. READ, *Untwisting the tetrahelix website*. <https://pubinv.github.io/tetrahelix/>, <https://pubinv.github.io/tetrahelix/> (accessed 2017-04-08).
- 558 [13] G. SADLER, F. FANG, J. KOVACS, AND K. IRWIN, *Periodic modification of the Boerdijk-Coxeter helix (tetrahelix)*, arXiv preprint arXiv:1302.1174, (2013), <https://arxiv.org/abs/1302.1174>.
- 559 [14] A. C. SANDERSON, *Modular robotics: Design and examples*, in Emerging Technologies and Factory Au-  
560 tomation, 1996. EFTA'96. Proceedings., 1996 IEEE Conference on, vol. 2, IEEE, 1996, pp. 460–466.
- 561 [15] S. SONG, D. KWON, AND W. KIM, *Spherical joint for coupling three or more links together at one point*,  
562 May 27 2003, <http://www.google.com/patents/US6568871>. US Patent 6,568,871.
- 563
- 564
- 565